

Monitoring Flood Driven Changes in Land Use Land Cover with Satellite Imagery

Anuradha M. Sangwai¹, Ajay D. Nagne²

^{1,2}Dr. G. Y. Pathrikar College of Computer Science and Information Technology, MGM University, Chhatrapati Sambhajanagar, Maharashtra, India.

Corresponding Author Email ID: anuradha.kulkarnid@gmail.com

ARTICLE INFO

ABSTRACT

Received: 31 Dec 2024

Revised: 20 Feb 2025

Accepted: 28 Feb 2025

Flood events significantly change the geographic distribution and extent of land use and land cover (LULC), with impacts on agriculture, barren land, built-up area, vegetation and water bodies. This study assesses LULC changes in the Krishna River basin, near Sangli district, Maharashtra, before and after the 2019 flood events using Landsat 8 OLI imagery for May 2019 (pre-flood) and October 2019 (post flood). LULC classification was carried out using the supervised classification approach using Maximum Likelihood technique, which ensures high precision in distinguishing between pre-flood and post-flood land cover types by using spectral information derived from training samples to assign each pixel to the most likely class. The accuracy of classified images was validated using ground truth data, accuracy assessment, including kappa statistics. The result indicates class- wise changes agricultural land expanded from 49.06% to 71% driven by rapid replanting, sediment deposition, enhanced soil moisture and barren land decreased from 12 % to 4%, while built-up areas reduced from 28% to 17% due to inundation. Vegetation showed a slight increase from 9% to 10% and water bodies remained constant at 1%, indicating that most floodwaters had receded. These changes illustrate both the destructive effects of inundation on built-up areas and the regenerative impacts on agriculture and vegetation. Results indicate substantial changes in LULC classes. The study demonstrates the effectiveness of integrating multi-temporal remote sensing with GIS tools to measure flood induced changes in land use and land cover. This approach offers significant contributions to disaster impact assessment, sustainable land management and rehabilitation in areas that are vulnerable to flooding.

Keywords: GIS, flood mapping, land use/land cover, maximum likelihood classification, remote sensing.

INTRODUCTION

Floods are among the most frequent and devastating natural events in the world, frequently causing major infrastructure damage, long-term economic disruption, and a high death toll. The monsoon season in India provides a prolonged heavy rainfall, which often resulting floods in a number of significant river basins [1]. One of the most notable river systems in India, the Krishna River Basin, is particularly vulnerable to these occurrences because of heavy monsoonal rainfall, dam releases, and unexpected changes in land usage [2]. A major hydrometeorological event, the 2019 flood caused extensive agricultural loss, urban inundation and ecological disturbance in Sangli district Maharashtra and adjoining locations within the basin. Planning for land use, environmental sustainability, and disaster preparedness all depend on an understanding of how such occurrences affect land systems [3]. The dynamic environmental indicators of land use and land cover (LULC) show both organic and agricultural changes. By drowning agricultural land, destroying built-up regions, and changing vegetation cover, floods drastically change LULC patterns [4]. Evaluating the amount of flood effect requires accurate monitoring and assessment of these changes. Remote Sensing (RS) and Geographic Information Systems (GIS) serve as powerful tools for analyzing

spatiotemporal variations in LULC in this context [5]. Regional-scale LULC mapping and change identification can benefit from multi-temporal, moderate-resolution data provided by satellite sensors like Landsat 8, which is equipped with the Thermal Infrared Sensor (TIRS) and Operational Land Imager (OLI) [6].

The effectiveness of LULC categorization and change detection methods in evaluating flood impacts has been shown in earlier research. Effective decision-making in post-disaster scenarios is supported by multi-temporal image analysis, which makes it easier to identify land cover changes, such as from barren ground to vegetation [7]. To produce precise thematic maps that differentiate between agriculture, barren land, built-up areas, vegetation and water bodies, the supervised classification techniques like support vector machines, maximum likelihood and random forest are frequently used [8]. The spatial and quantitative number of flood-induced changes can then be revealed by comparing these classed maps using change detection techniques.

The Krishna River Basin, while agriculturally productive and densely inhabited, is increasingly vulnerable to floods due to deforestation, urban sprawl and encroachments in low-lying floodplains. The 2019 flood event offers a valuable opportunity to assess how extreme hydrological stressors affect land systems in such complex and sensitive environments [9][10]. Therefore, using Landsat 8 satellite imagery, the current work attempts to examine the temporal changes in land use and land cover brought on by the 2019 flood in the basin of Krishna River. LULC maps are created in a GIS environment using supervised classification approaches for two time periods: May 2019 (pre-flood) and October 2019 (post-flood). In order to assess the scope and character of LULC transitions, the classified maps are compared. Changes in vegetation, built-up areas, agricultural and barren land are given special attention. It is anticipated that the findings will advance knowledge of the effects of flooding and aid in the creation of better land-use policies, flood risk management strategies and plans for sustainable development in areas vulnerable to flooding.

STUDY AREA

The study area is situated in the Sangli district of Maharashtra, India, a region that experienced severe flooding during August 2019. Geographically, it lies between approximately 16°45'N to 17°15'N latitude and 74°15'E to 74°45'E longitude, covering fertile floodplains along a major river system. The tropical monsoon climate, receiving most of its rainfall occurring from June to September. Sangli district is characterized by fertile rich alluvial soils, which supports intensive agriculture practices. However, its location within a low-lying floodplain and closeness to major river channels makes it extremely prone to flooding during heavy rainfall events and upstream water releases [11]. The August 2019 flood submerged vast agricultural areas, damaged built-up zones, and altered land cover patterns. The district contains diverse land cover types, including water bodies, agricultural land, built-up areas, vegetation and barren land making it appropriate for detailed multi-temporal LULC change detection and flood effect assessment through remote sensing techniques and geographic information techniques. The figure 1 shows location of study area. The Krishna River basin is the second largest in Sangli district, Maharashtra. It rises in Western Ghats, Maharashtra and flows east and passes through Sangli district. The river runs 301 kilometers through this state. It is usual for the river to meander when it traverses plains. Consequently, the Krishna River has many turns and tribulations. Curves and meanders significantly reduce the velocity, which increases flooding on both the inner and outer banks. The selection of the study area should consider factors including geographic constraints, land use, size and the existence of significant rivers [12].

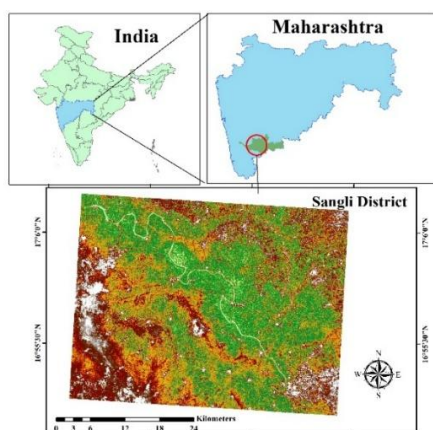


Fig. 1: Location of the Study Area.

METHODOLOGY

A systematic series of remote sensing and GIS-based techniques were used in the present work methodology, to determine and evaluate changes in land use and land cover (LULC) brought on by the 2019 flood in the Krishna River Basin. The methodology consisted of six main stages: satellite image acquisition, image preprocessing, supervised classification, area computation, accuracy assessment, and final LULC map generation [13]. Below is a detailed description of each stage as shown in figure 2.

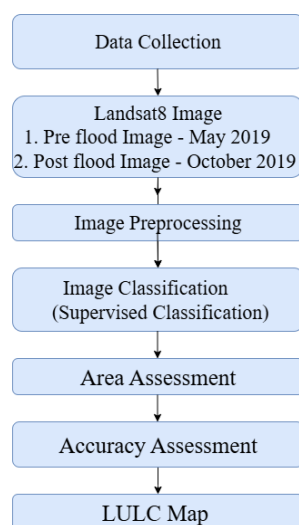


Fig. 2: Methodology Adopted.

DATA COLLECTION

This study made use of multi-temporal Landsat 8 OLI satellite data. One image from the pre-flood period May 2019 and another from the post-flood October 2019 period were obtained. Regional-scale LULC investigations can benefit from the multispectral imagery that Landsat 8 offers, which has a resolution of 30 meters [14]. The satellite imagery for the study was obtained from the USGS Earth Explorer.

IMAGE PRE-PROCESSING

To get the satellite data ready for analysis, typical image preprocessing was used before classification. A multispectral composite image was first produced by layer stacking using the appropriate spectral bands 1 to 7. Spatial correctness was then ensured by georeferencing and projecting the data using the WGS 84 datum to the Universal Transverse

Mercator (UTM) coordinate system, Zone 43N [15]. The analysis was then confined to the specific study area by extracting the region of interest, which is a section of the Krishna River Basin, using a shapefile.

IMAGE CLASSIFICATION

This study primarily utilized the Maximum Likelihood classification approach to map and analyze modifications in land use and land cover (LULC). This supervised classification method was selected due to its solid statistical foundation, which allows each pixel in a remote sensing image to be assigned to the class for which it has the best likelihood of belonging based on spectral values [16]. Utilizing satellite imagery from May 2019 (before to the flood) and October 2019 (post-flood), temporal variations in LULC were identified and recorded. The Landsat8 images included in the datasets has several spectral bands that may be used for in-depth classification [17]. Training samples were developed using a combination of visual interpretation and prior information of the study area for the five main land cover classes (agricultural, barren land, built-up area, vegetation, and water bodies) before categorization shown in Table 1. Its suitability for this study was validated by the MLC algorithm which demonstrated high accuracy and reliability for Landsat-based LULC mapping.

Table 1: Land cover Classification

Sr. No.	Land Cover	Description
1.	Agriculture	Land cover crop field, fallow, plantation
2.	Barren Land	Land cover by residential, commercial services, building & other man-made structure, industrial area, mixed built up land
3.	Built-up Area	Land with sand, rocks, bare ground, gravel pits, strips mines
4.	Vegetation	Lands with trees, scattered plants, forest land
5.	Water Body	River, reservoir, lakes, streams

AREA ASSESSMENT

Using GIS-based analysis the area corresponding to each land cover category was calculated after classification and expressed in square kilometers of the total study area. The ability to compare LULC categories quantitatively between May and October 2019 highlighted transitions brought on by floods.

ACCURACY ASSESSMENT

An accuracy assessment was conducted using reference points gathered from high quality Google Earth images. To evaluate the dependability of the categorized LULC maps, a confusion matrix was generated and the user's accuracy, producer's accuracy, kappa coefficient and total accuracy were calculated [18][19].

LULC MAP

Final land use land cover maps were created for both the pre and post flood areas. Major land cover changes, especially the effects of flooding on agricultural land, populated regions and barren land were identified and quantified through the analysis and interpretation of the generated maps.

RESULTS AND DISCUSSION

The land use land cover maps for the study area were developed using maximum likelihood classification approach. LULC maps classified into five categories: agriculture, barren land, built-up area, vegetation and water body.

LAND USE LAND COVER CLASSIFICATION PRE-FLOOD

The pre-flood LULC classification for May 2019, generated using the Maximum Likelihood Classification technique on Landsat 8 imagery, revealed five major land cover categories: Agriculture, Barren Land, Built-up Area, Vegetation and Water Body. Areal statistics show that Agriculture was the dominant class, occupying 49.06% (819.41 km²) of the total study area, followed by Built-up Area at 28.41% (474.85 km²). Barren Land covered 12.41% (207.35 km²), while Vegetation accounted for 9.06% (157.80 km²). Water Bodies were limited to 1.06% (11.00 km²), as expected

during the pre-monsoon period when river discharge is minimal. The classification achieved an overall accuracy of 82% with a Kappa coefficient of 0.6959, indicating substantial agreement between classified and reference data.

Table 2: The Area wise distribution of LULC of pre-flood image

Sr No.	LULC Class	Area (km ²)	Area (%)
1.	Agriculture	819.41	49.06
2.	Barren Land	207.35	12.41
3.	Built-up Area	474.85	28.41
4.	Vegetation	157.80	9.06
5.	Water Body	11.00	1.06
6.	Total	1670.41	100

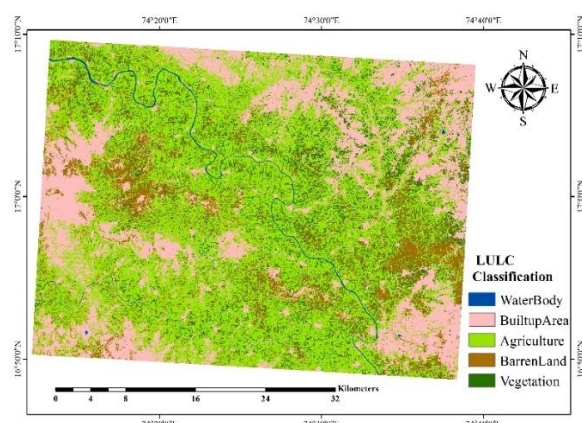


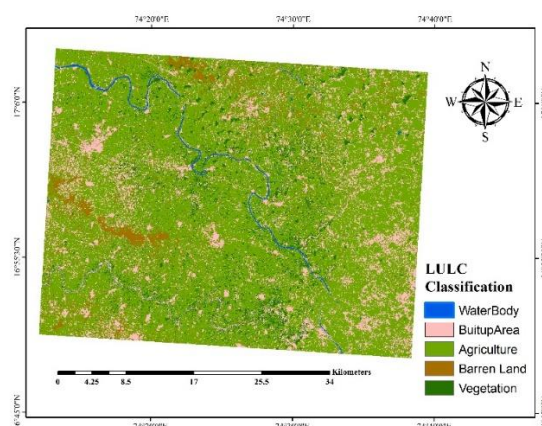
Fig. 3: Pre-flood LULC Classification.

LAND USE LAND COVER CLASSIFICATION POST FLOOD

The post-flood LULC classification for October 2019 indicates significant spatial changes in land cover following the flood event. Agriculture increased sharply to 71% (1182.47 km²), reflecting extensive water recession and renewed cropping activity after the floods. Built-up Area declined to 17% (289.78 km²), possibly due to inundation effects. Barren Land reduced drastically to 4% (73.58 km²), while Vegetation slightly increased to 10% (109.38 km²). The Water Body class remained at 1% (15.20 km²), though its spatial distribution expanded along river courses, consistent with post-flood high water retention in certain pockets. The classification attained an overall accuracy of 90% and a Kappa coefficient of 0.7374, demonstrating improved post-flood classification reliability compared to pre-flood mapping. These changes underline the significant hydrological and geomorphological influence of the flood on land cover distribution. The reduction in barren land and built-up areas, alongside an increase in agriculture, points towards post-flood land use adjustments and short-term rehabilitation efforts.

Table 3. The area wise distribution of LULC of post flood image

Sr. No.	LULC Class	Area (km ²)	Area (%)
1.	Agriculture	1182.47	71
2.	Barren Land	73.58	4
3.	Built-up Area	289.78	17
4.	Vegetation	109.38	10
5.	Water Body	15.20	1
6.	Total	1670.41	100

**Fig. 4:** Post-flood LULC Classification.

LAND USE LAND COVER CHANGE DETECTION

The study area's land use and land cover maps for May 2019 figure 3 and October 2019 figure 4 were created using satellite imagery. These maps show how different land types, such as agricultural, barren land, built up area, vegetation and water bodies are distributed spatially. Land cover variations over time were examined by comparing satellite imagery. This methodology enabled the measurement of improvement and decrease in each land use class and made it easier to identify changes in land cover categories. In order to identify trends and patterns in LULC changes the classification and change detection analysis results were evaluated. Table 4 The pre flood and post flood LULC maps provide a clear visual and quantitative evaluation of flood impacts in the study area. The observed agricultural expansion post-flood highlights the resilience of rural communities and the benefits of flood-deposited alluvium, which can enhance soil fertility. However, the decline in built-up area coverage may indicate both actual flood-induced damage to infrastructure and classification limitations in distinguishing between damaged settlements and agricultural/barren land. Overall, the change detection analysis offers important insights into flood-induced land cover transformations, supporting disaster impact assessment and informing future flood management strategies in the Krishna River basin.

Table 4: LULC change detection

LULC Class	May-2019 Area (%)	October 2019 Area (%)	Change (%)	Change Description
Agriculture	49	71	+22	Significant increase due to flood water recession
Barren Land	12	4	-8	Large reduction as barren land converted to agriculture or flood water
Built-up Area	28	17	-11	Decrease due to inundation, damage to settlement
Vegetation	9	10	+1	Vegetation cover increased, possibly due to seasonal agricultural activities and regeneration after flood recession.
Water Body	1	1	0	Spatial distribution expanded along river channels and floodplain

ACCURACY ASSESSMENT

In remote sensing, the Kappa coefficient is a commonly used statistical measure to assess how accurately land use and land cover classifications are made. It considers the agreement that might occur by default and measures the agreement between reference data and classified data. The Kappa coefficient is therefore a reliable instrument for evaluating the accuracy of classification findings. Using the Kappa coefficient and additional measures like producer's

accuracy, user's accuracy and overall accuracy, it can improve the validity and reliability of classifications based on remote sensing [20][21]. By including these measures, categorization performance may be thoroughly assessed. pre-flood and post flood LULC classification, generated using the Maximum Likelihood Classification technique on Landsat 8 imagery, revealed five major land cover categories: Agriculture, Barren Land, Built-up Area, Vegetation and Water Body.

CONCLUSION

The Significant flood driven variations in land use and land cover were detected in the Sangli district after a multitemporal assessment of satellite images from May 2019 (pre-flood) and October 2019 (post-flood) that was categorized using the supervised maximum likelihood approach. The result indicates class-wise changes agricultural land expanded from 49.06% to 71% driven by rapid replanting, sediment deposition, enhanced soil moisture and barren land decreased from 12 % to 4%, while built-up areas reduced from 28% to 17% due to inundation. Vegetation showed a slight increase from 9% to 10% and water bodies remained constant at 1%, indicating that most floodwaters had receded. These findings show how significant hydrological events may quickly alter floodplain environments, highlighting both the destructive and restorative effects of the 2019 flood. The results emphasize the importance of integrating remote sensing and GIS for prompt post-disaster evaluation, which can aid in resilience planning, disaster preparedness and sustainable land management.

REFERENCES

- [1] Abayneh, T. G., Ephrem, G. & Hayal, D., (2024) GIS and Remote sensing-based land use land cover change classification map, interlinked with population growth dynamics in Awash River Basin (ARB), Ethiopia. at <https://doi.org/10.21203/rs.3.rs-4528962/v>
- [2] Abebe, G., Getachew, D. & Ewunetu, A.,(2022) Analysing land use/land cover changes and its dynamics using remote sensing and GIS in Gubalafito district, Northeastern Ethiopia. SN Appl. Sci. 4, 30. <https://doi.org/10.1007/s42452-021-04915-8>
- [3] Arveti N., Etikala B., and Dash P. (2016) Land Use/ Land Cover Analysis Based on Various Comprehensive Geospatial Data Sets: A Case Study from Tirupati Area, South India, Advances in Remote Sensing, 05(02): 73-82. <https://doi.org/10.4236/ars.2016.52006>.
- [4] Bill Donatien, L. M., Clobite, B. B. & Meris Midel, M. L. ,(2024) Land use land cover change detection using multi-temporal Landsat imagery in the North of Congo Republic: a case study in Sangha region. Geocarto International 39. <https://doi.org/10.1080/10106049.2024.2425184>
- [5] B V Ramanamurthy and N Victorbabu (2021) Land Use Land Cover (LULC) classification with wasteland demarcation using Remote sensing and GIS Techniques. IOP Conf. Ser.: Mater. Sci. Eng. 1025 012035 DOI 10.1088/1757-899X/1025/1/012035.
- [6] Chaikaew, P. (2019). Land Use Change Monitoring and Modelling using GIS and Remote Sensing Data for Watershed Scale in Thailand. IntechOpen. DOI: <http://dx.doi.org/10.5772/intechopen.79167>.
- [7] Kafi, K. M., Shafri, H. Z. M. & Shariff, A. B. M., (2014) An analysis of LULC change detection using remotely sensed data; A Case study of Bauchi City. in IOP Conference Series: Earth and Environmental Science vol. 20 (Institute of Physics Publishing) DOI : 10.1088/1755-1315/20/1/012056
- [8] Kumar, G., Sahoo, R. N. & Sehgal, V. K., (2008) Land Use Land Cover Change in Active Flood Plain using Satellite Remote Sensing. Jour. Agric. Physics vol. 8 <https://www.researchgate.net/publication/265421597>.
- [9] Kumari, A. et al.,(2021) Decadal Land Use Land Cover Change Analysis using Remote Sensing and GIS in Nagpur city of Maharashtra, India. JOURNAL OF AGRISEARCH 9, 265-269. <https://doi.org/10.21921/jas.v9i03.11013>
- [10] Mohan Rajan, S. N., Loganathan, A. & Manoharan, P.,(2020) Survey on Land Use/Land Cover (LU/LC) change analysis in remote sensing and GIS environment: Techniques and Challenges. Environmental Science and Pollution Research vol. 27 29900-29926 . <https://doi.org/10.1007/s11356-020-09091-7>.
- [11] Mangan, P, Rajgopal N, Shaktivel G, Amrutha D.E., (2014) Land Use and Land Cover Change Detection Using Remote Sensing and GIS in Parts of Coimbatore and Tiruppur Districts, Tamil Nadu, Indis. International Journal of Remote Sensing & Geoscience (IJRSG) vol 3,issue 1, 15-20.

- [12] Mane, R., Patil, M., Wandre, S. & Dalavi, P., (2024) Preparation of Land Use Land Cover (Lulc) for Panchganga River Basin Using Remote Sensing and GIS. at <https://doi.org/10.21203/rs.3.rs-4529737/v1>.
- [13] Mousavi, S. M., Roostaei, S. & Rostamzadeh, H., (2019) Estimation of flood land use/land cover mapping by regional modelling of flood hazard at sub-basin level case study: Marand basin. *Geomatics, Natural Hazards and Risk* 10, 1155–1175. <https://doi.org/10.1080/19475705.2018.1549112>
- [14] Rawat, J. S. & Kumar, M., (2015) Monitoring land use/cover change using remote sensing and GIS techniques: A case study of Hawalbagh block, district Almora, Uttarakhand, India. *Egyptian Journal of Remote Sensing and Space Science* 18, 77–84. <https://doi.org/10.1016/j.ejrs.2015.02.002>
- [15] Reis, S.,(2008) Analyzing land use/land cover changes using remote sensing and GIS in Rize, North-East Turkey. *Sensors* 8, 6188–6202 (2008). <https://doi.org/10.3390/s8106188>
- [16] Rujoiu-Mare, M.-R. & Mihai, B.-A. (2016) Mapping Land Cover Using Remote Sensing Data and GIS Techniques: A Case Study of Prahova Subcarpathians. *Procedia Environmental Sciences* 32, 244–255. <https://doi.org/10.1016/j.proenv.2016.03.029>
- [17] Rwanga, S. S. & Ndambuki, J. M., (2017) Accuracy Assessment of Land Use/Land Cover Classification Using Remote Sensing and GIS. *International Journal of Geosciences* 08, 611–622. doi: [10.4236/ijg.2017.84033](https://doi.org/10.4236/ijg.2017.84033).
- [18] Sugianto, S., Deli, A., Miswar, E., Rusdi, M. & Irham, M.,(2022) The Effect of Land Use and Land Cover Changes on Flood Occurrence in Teunom Watershed, Aceh Jaya. *Land* 11. <https://doi.org/10.3390/land11081271>
- [19] Seyam, M. M. H., Haque, M. R. & Rahman, M. M.,(2023) Identifying the land use land cover (LULC) changes using remote sensing and GIS approach: A case study at Bhaluka in Mymensingh, Bangladesh. *Case Studies in Chemical and Environmental Engineering* 7. <https://doi.org/10.1016/j.cscee.2022.100293>.
- [20] S. S. Shinde et al.,(2024) Temporal and Spatial Dynamics of Land Use and Land Cover in Shirur Kasar Tehsil, Maharashtra Using Geospatial Technology. *International Journal of Agricultural Invention* 9, 193–204. <https://doi.org/10.46492/IJAI/2024.9.1.25>
- [21] Singh, R. K. et al. (2018) Land use/land cover change detection analysis using remote sensing and GIS of Dhanbad district, India. *Eurasian Journal of Forest Science* 6, 1–12. <https://doi.org/10.31195/ejefsf.428381>